

HADRONIC INTERACTIONS AT LOW  $p_T$ \*

BY A. CAPELLA

Laboratoire de Physique Théorique et Hautes Energies, Université Paris-Sud, Orsay\*\*

(Received October 22, 1982)

The mechanism of multi-hadron production in low  $p_T$  hadronic interactions is studied in the framework of the dual parton model. The predictions of the model are compared with recent experimental data on pp and  $\bar{p}p$  collisions at ISR and SPS colliders,  $\bar{p}p$  annihilation, proton-nucleus collisions,  $\alpha-\alpha$  collisions at ISR, etc. I also review some predictions of the reggeon calculus for  $\sigma_{\text{Tot}}$  and  $d\sigma/dt$ , as well as the dual model approach to the calculation of hadronic masses.

PACS numbers: 13.85.-t

## 1. Introduction

In hadronic interactions the low  $p_T$  events represent more than 99% of all events. One of its most spectacular features is the production of lots of hadrons — the average multiplicity at the CERN-SPS colliders is about 40, with events containing more than one hundred particles. We would like to understand how these particles are produced. This involves two different although related questions

a) what is the mechanism responsible for multi-hadron production? Is it analogous to a  $q-\bar{q}$  separation, or more generally a  $3-\bar{3}$  color separation, as in  $e^+e^-$  or deep inelastic lp scattering or is it something very different?

b) What are the properties of the hadronic system produced via this mechanism? i.e. What are the properties of hadronization?

We believe that QCD is the theory of strong interactions — not only large  $p_T$  or hard interactions but also soft ones since there is only one QCD. Thus we should ask first of all what does QCD tell us about questions a) and b). The answer is: very little, at least for soft processes. For hard ones it provides an answer to question a) but again it tells us very little about question b).

---

\* Presented at the XXII Cracow School of Theoretical Physics, Zakopane, May 30- June 9, 1982.

\*\* Address: Laboratoire de Physiques Théoriques et Hautes Énergies, Batiment 211, Université Paris XI, Centre d'Orsay, 91405 Orsay, France.

## 2. Hard processes

Let us first review very briefly the situation for hard processes. All of us can draw the (perturbative) QCD diagrams responsible for hadron production in say  $e^+e^-$  annihilation, deep inelastic lp scattering or Drell-Yan processes. These diagrams provide an answer to question a). What about question b)? For definiteness let us consider  $e^+e^-$  annihilation (Fig. 1). At large  $Q^2$  the  $q$  and  $\bar{q}$  are very far off-shell and perturbative QCD applies ( $\alpha(Q^2)$

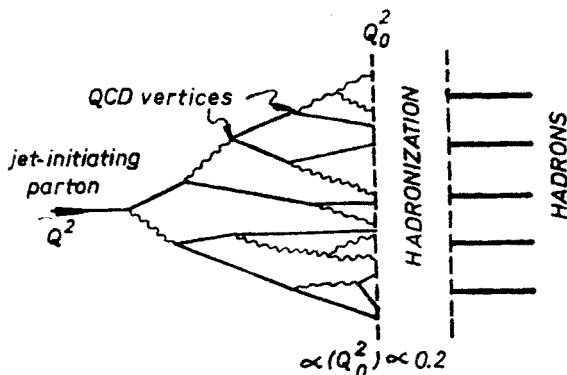


Fig. 1. Perturbative ( $Q^2 > Q_0^2$ ) and non-perturbative ( $Q^2 < Q_0^2$ ) stages of the process  $e^+e^- \rightarrow \text{hadrons}$

$\ll 1$ ). A repeated branching takes place via the QCD vertices:  $q \rightarrow q + g$ ,  $g \rightarrow q + \bar{q}$  and  $g \rightarrow g + g$ . As a consequence of this branching, many partons are produced at lower momenta which are less far off-shell. When this off-shellness reaches a value  $Q^2 = Q_0^2$  such that  $\alpha(Q_0^2)$  is no longer small, one enters into a non-perturbative regime. The exact value of  $Q_0^2$  is not known, presumably it is in the range of 1 to 10  $\text{GeV}^2$ . From  $Q^2$  to  $Q_0^2$  the process is entirely calculable in perturbative QCD (using, for instance, the jet calculus formalism [1]). One obtains:

$$\langle n \rangle \sim \exp(c \sqrt{\ln Q^2}), \quad \langle p_T^2 \rangle \sim Q^2. \quad (1)$$

However these properties refer to a partonic system and not to hadrons. The hadronization takes place in the nonperturbative regime. As emphasized by Politzer in his talk at the Paris Conference, all models for hadronization not only are not QCD but they are not quantum field theoretical or even quantum mechanical models. They are just classical models (recursive cascade model, string models etc.) [2]. Thus although these models are quite successful phenomenologically, one should keep in mind this severe theoretical limitation.

The discussion above can be summarized in the following formula for the fragmentation function (obtained [2] in models of the fragmentation type):

$$D_{i \rightarrow h}(x, Q^2) = \sum_a \int_x^1 \frac{dx'}{x'} D_{i \rightarrow a}(x', Q^2, Q_0^2) \cdot D_{a \rightarrow h}\left(\frac{x}{x'}\right). \quad (2)$$

Here  $D_{i \rightarrow a}$  describes the fragmentation of a parton  $i$  at  $Q^2$  into another parton  $a$  at a lower value  $Q_0^2$  and carrying a fraction  $x'$  of the longitudinal momentum of  $i$ . This function is calculable in perturbative QCD. The conversion of parton  $a$  into a hadron is described by  $D_{a \rightarrow h}$ . This part is computed with a classical model.

It has been argued by Amati and Veneziano [3] that hadronization is essentially harmless in the sense that it does not change the results in Eq. (1), obtained in perturbative QCD. This is presumably true only for ultra large values of  $Q^2$ . For the ones available in present experiments, the non-perturbative part seems to be dominant.

I will not extend this general discussion any further. Some recent developments in the field (both theoretical and experimental) include baryon production in quark jets and diquark jets [2].

Let me conclude this introduction by mentioning a very interesting property of quark and diquark jets. All experiments tend to indicate that these jets are universal. By this I mean that the nonperturbative part of the fragmentation function of a quark (or diquark) of a given flavor is the same in all reactions (hard or soft). This jet universality will be extensively used in what follows.

### 3. Low $p_T$ (soft) hadron-hadron interactions

Here we are from the very beginning in a non-perturbative regime and QCD does not even provide an answer to question a). The different models available propose different mechanisms of hadron production. Among these models we have:

- the well known Additive Quark Model (AQM) [4a]. The recombination models in their most recent form (“valon model” [4b]) are of this type;
- the perturbative QCD models. They are based on ideas due to Low and Noussinov [5]. Extensive calculations in this model have been performed recently [6];
- the Lund fragmentation model which is based on a classical string model [7];
- the dual parton model [8] based in the  $1/N$  expansion in DTU (Dual Topological Unitarization) [9];
- the Massive Quark Model (MQM) introduced by Preparata [10]. Although very different in spirit from the previous models, it has some similarity with the dual parton model in its final formulation.

I will discuss now in some detail the dual parton model.

The underlying idea of the dual parton model is of a very general nature: since the coupling constant  $g$  is not small and a perturbative expansion in powers of  $g$  does not make sense, one should try and find another parameter which would allow some kind of perturbative treatment. It turns out that the topology of a diagram (described by standard topological parameters) allows such a perturbative treatment [11]. Indeed, the diagrams with simple topological properties dominate over the ones with a more complicated topology, since by complicating the topology of a graph, its contribution to, say,  $\sigma_{\text{tot}}$  is depressed by powers of  $1/N^2$  (here  $N$  represents either the number of flavors or the number of colors).

The dominant diagram at high energy (Pomeron) is shown in Fig. 2. Two chains or strings of hadrons are produced (one chain = two back-to-back jets). All chains are

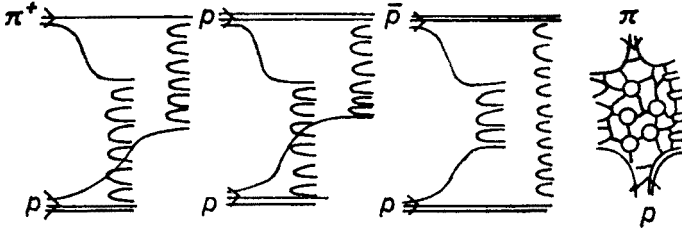


Fig. 2. The dominant production graphs for  $\pi$ - $p$ ,  $p$ - $p$  and  $\bar{p}$ - $p$  interactions. A summation over quark loops and gluons (shown only in the last graph) is implicitly assumed. More precisely, the first graph is identical to the fourth one, after performing such a summation

of three types  $q-\bar{q}$ ,  $qq-q$  and  $qq-\bar{q}\bar{q}$ . The color balance is reached via gluon exchange (presumably a complicated fishnet of gluons and quark loops, since we are in a non-perturbative regime). This diagram is of order  $1/N^2$ . Notice that as a consequence of the interaction the meson splits into its  $q$  and  $\bar{q}$  valence quarks and a baryon into  $q$  and  $qq$ .

The next-to-leading diagram ( $P-P$  cut) is shown in Fig. 3. It is of order  $1/N^4$ . In this case four chains of hadrons are produced. All chains belong to one of the three previous types except that in this case some of the chains involve  $q$  and  $\bar{q}$  from the sea. Here the hadron splits into four colored systems, i.e. the interaction picks up a fluctuation in the hadron wave function consisting, in the case of a proton, in  $q_v$ ,  $(qq_v)$ ,  $q_s$ ,  $\bar{q}_s$ . Likewise, the terms of order  $1/N^6$  will contain six chains of hadrons, etc.

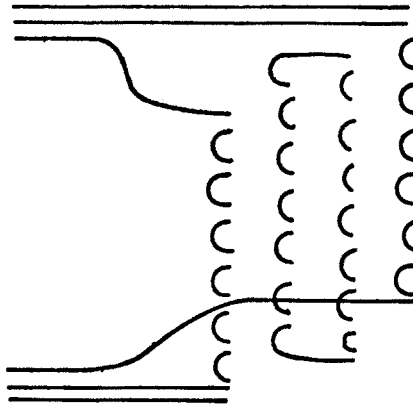


Fig. 3. Example of a four-chain (non-dominant) production graph in  $p$ - $p$  interactions

Of course, this is not QCD. However, these topological arguments are very general and might be true in any theory. In fact, the  $1/N$  expansion, in which they are based, provides a conceptual link between Dual and Gauge theories [11]. There is also a one to one correspondence between the various orders in the  $1/N$  expansion and unitarity corrections. Thus, the terms in  $1/N^2$  correspond to a single interaction; the terms in  $1/N^4$  contain a rescattering in either the initial or final state, etc. A link with the reggeon field theory is obtained in this way [11].

In order to make the dual parton model quantitative, one needs the three following ingredients:

a) the momentum distribution function giving the probability that each chain has a certain invariant mass. It can be obtained from the very general features of the model (dominance of standard regge singularities). It turns out [8] that in the case of a proton the valence quarks are slow in the average and the sea quarks even slower (with  $1/\sqrt{x}$  and  $1/x$  distributions near  $x \approx 0$ , respectively). On the contrary, the diquark is fast in the average since the sum of the  $x$ -values of all constituents is equal to one<sup>1</sup>.

b) the fragmentation functions of the constituents at the ends of the various chains, or, in other words, the properties of the hadrons produced in each chain for fixed  $x$ -values of the constituents at its two ends. These are *not* given by the model. One has to use the classical models referred to above or use the jet universality hypothesis.

c) the relative weights of the contributions corresponding to successive orders in the  $1/N$  expansion. They are given by the eikonal or perturbative reggeon field theory for hadron-hadron interactions and by the Glauber-Gribov formulae in the case of interactions on a nuclear target.

The model is thus completely specified. With jet universality assumed, one can compute all the properties of the hadronic system produced in a hadron-hadron collision (rapidity distributions, multiplicity distributions, etc.) with no free parameter, using as an input the corresponding quantities as measured in hard processes — no freely adjustable parameter is involved.

Before giving the numerical results and their comparison with experimental data let me tell you what are the qualitative features of the model. To be specific I will consider the charged particle rapidity distributions in a pp inclusive reaction. As explained above, the main component (Pomeron) contains two chains stretched from a (fast) diquark of one proton to a (slow) quark of the other proton (Fig. 2). The non-leading contributions will contain these two chains plus an even number of extra chains stretched between sea quarks and antiquarks (Fig. 3). The resulting pp rapidity distribution will be obtained by adding all these contributions with appropriate weights<sup>2</sup>. The pp central plateau will

<sup>1</sup> The exact form of the momentum distribution function for a proton is [8c]

$$e_{2\mu}^p(x_1^{qv}, x_2^{qs}, \dots, x_{2\mu}^{qq}) = C_\mu \frac{1}{\sqrt{x_1^{qv}}} \frac{1}{x_2^{qs}} \dots (x_{2\mu})^{3/2} \delta(1 - x_1^{qv} - x_2^{qs} - \dots - x_{2\mu}^{qq}).$$

Here  $x_1$  refers to the valence quark,  $x_{2\mu}$  to the diquark and  $x_2, \dots, x_{2\mu-1}$  to the sea quarks and antiquarks.  $C$  is determined from the normalization to 1 of the probability functions  $e_{2\mu}$ . For a pion one has instead [8c]

$$e_{2\mu}^\pi(x_1^{qv}, x_2^{qs}, \dots, x_{2\mu}^{\bar{q}v}) = C_\mu \frac{1}{\sqrt{x_1^{qv}}} \frac{1}{x_2^{qs}} \dots \frac{1}{\sqrt{x_{2\mu}^{\bar{q}v}}} \delta(1 - x_1^{qv} - x_2^{qs} - \dots - x_{2\mu}^{\bar{q}v}).$$

<sup>2</sup> One has [8d]

$$\frac{dN^{pp}}{dy} = \frac{1}{\sigma_{in}} \sum_\mu \sigma_\mu \left[ \frac{dN^{(qq)1-q_2}}{dy} + \frac{dN^{q_1-(qq)2}}{dy} + (2\mu-2) \frac{dN^{q-\bar{q}}}{dy} \right]$$

with  $\sum_\mu \sigma_\mu = \sigma_{in}$ . Indeed, a diagram with  $2\mu$  chains (with weight  $\sigma_\mu$ ) contains two  $(q-q\bar{q})$  chains and the remaining  $2\mu-2$  ones are  $(q-\bar{q})$  chains. The  $dN/dy$  of each chain is given by convolutions of the momentum distribution functions  $\varrho$  with appropriate fragmentation functions — as in the parton model. Here however there is an extra kinematical complication due to the fact that the C. of M. of a chain does not coincide with the overall C. of M.

rise with  $s$  due to two effects. First there will be an increasing overlap between the two main chains; second at low energies the  $q-\bar{q}$  chains are very narrow and of a negligible height due to phase space limitation; at ultra-high energies, however, they will develop full size plateaus. Since these extra  $q-\bar{q}$  chains are narrow and centered at  $y^* = 0$ , the width of the pp rapidity distribution will increase with  $s$  less rapidly than expected from the increase in  $Y_{\max}$ .

Calculations of  $\langle n \rangle$  and  $dn/dy$ , including the multi-chain components were performed by Capella and Tran [8d] and independently by Aurenche and Bopp [12] using an identical model. Recently calculations in a similar but not identical model by Kaidalov and Ter-Martirosyan have appeared in the literature [13]. The results, borrowed from Ref. [8d], are presented in Figs. 4, 5 and 6. Charge distributions have been computed in the Dual Parton Model by Pagnamenta and Sukhatme [14].

The second moments of the rapidity distributions, using as an input the  $D/\langle n \rangle$  ratios in  $e^+e^-$  and lp scattering, have also been computed [8d, 15a] (in the latter using the two-chain component only). One obtains a  $D/\langle n \rangle$  ratio appreciably larger than in  $e^+e^-$  and approximately constant up to  $\sqrt{s} = 540$  GeV. This is in rough agreement with KNO scaling. On the other hand in Ref. [13b] the topological cross-section were computed assuming a Poisson distribution for the particles produced in each chain. The authors find a rather large violation of KNO scaling between ISR and CERN SPS energies, which turns out to be inconsistent with present data [16]. Although the dual parton model does not have exact KNO scaling, such a large violation seems to me rather surprising.

The multi-chain components in the model produce a (long-range) forward-backward correlation — even if one assumes short-range order for the particles produced in each chain [17]. The most sensitive measure of this correlation is the slope parameter:

$$b_{\text{outer}} \equiv \frac{d\langle n_B \rangle}{dn_F} = \frac{\langle n_F n_B \rangle - \langle n_F \rangle \langle n_B \rangle}{\langle n_B^2 \rangle - \langle n_B \rangle^2} \quad \text{in the "outer" region (i.e. excluding the particles produced in the range } -1 < \eta < +1). \quad b_{\text{outer}} = 0 \text{ means that there are no long}$$

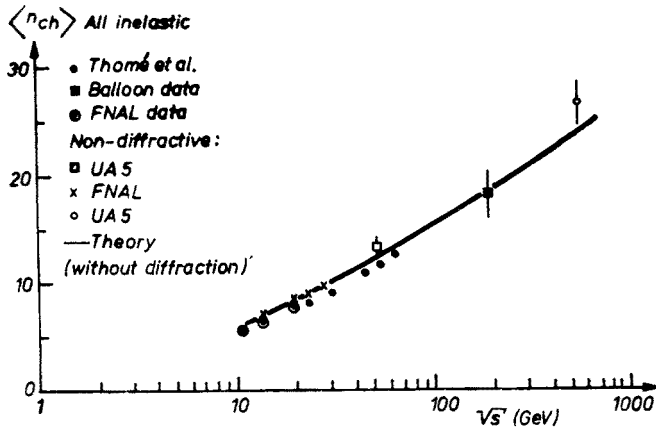


Fig. 4. The average pp charged multiplicity compared with experimental data. The theoretical value of the pp multiplicity, at  $\sqrt{s} = 540$  GeV is only 1% higher

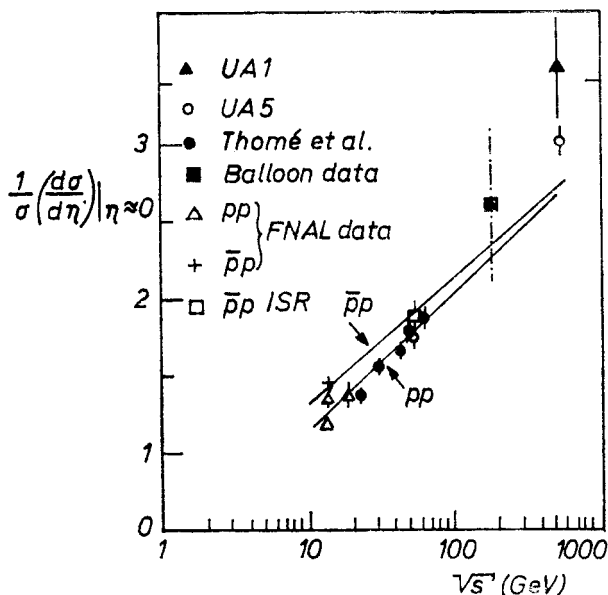


Fig. 5. The central plateau height  $(1/\sigma)(d\sigma/dy)$  ( $y^* = 0$ ) compared with the preliminary experimental data  $(1/\sigma)(d\sigma/d\eta)$  ( $\eta^* = 0$ ). The comparison is meaningful since the ratio of these two quantities is expected to be roughly independent of  $s$ . The theoretical curve has been normalized to the experimental data at  $\sqrt{s} = 20$  GeV

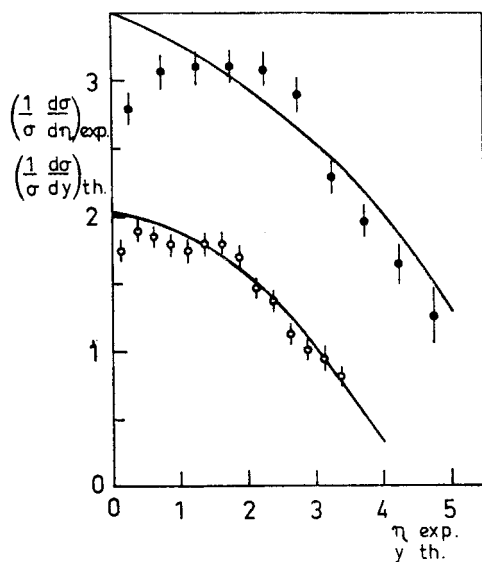


Fig. 6. Charged particle distributions at  $\sqrt{s} = 53$  and  $540$  GeV compared with data on  $(1/\sigma)d\sigma/d\eta$  [19]. The curve at  $540$  GeV has the absolute normalization predicted by the model. The curve at  $53$  GeV has been lowered by  $15\%$  — the rise in the plateau given by the model being smaller than the experimental one by  $\sim 15\%$  (see Fig. 5)

range correlations;  $b_{\text{outer}} \neq 0$  means a correlation between particles separated from each other by more than two units (long-range). Theoretically, the assumption of short range order within a chain implies that each individual chain gives  $b_{\text{outer}} = 0$ . Therefore  $b_{\text{outer}}$  can be computed in the dual parton model without using any input from hard scattering. One obtains [18]

$$\langle n_F n_B \rangle - \langle n_F \rangle \langle n_B \rangle \sim 4 D_\mu^2 \langle n_{q-\bar{q}} \rangle$$

where  $D_\mu^2 = \langle \mu^2 \rangle - \langle \mu \rangle^2$  is the dispersion in the number of chains and  $\langle n_{q-\bar{q}} \rangle$  is the average charged multiplicity of a  $q-\bar{q}$  chain. This gives  $b_{\text{outer}} (\sqrt{s} = 540) = 0.3 \div 0.4$ . The experimental value is 0.4 [19]. Most of the observed forward-backward correlation can be explained by the fluctuation in the number of chains.  $b_{\text{outer}}$  has also been computed by Fiałkowski and Kotański [15b] up to ISR energies using the two-chain component only.

#### 4. $\bar{p}-p$ annihilation

We turn next to  $\bar{p}p$  annihilation, a topic particularly relevant to the subject of this meeting. In the dual parton model the appropriate diagram is shown in Fig. 7. The hadronic system is produced in the form of three  $q-\bar{q}$  chains. Note that by splitting the diquark into its two quarks, which fragment independently, no leading baryon is produced. The contribution of such a diagram to  $\sigma_T$  goes to zero when  $s$  increases (as  $1/\sqrt{s}$ ). As in the non-annihilation cases discussed above one has also higher order contributions in the  $1/N$  expansion which contain the three chains in Fig. 7 plus an even number of chains linking

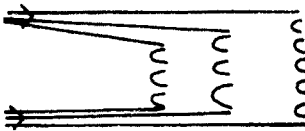


Fig. 7. Dual graph for  $\bar{p}-p$  annihilation

sea quarks and antiquarks. The fragmentation functions are, of course, the same as in the non-annihilation case, and the momentum distribution functions can again be computed from the model. Here one has, for the diagram with only three chains

$$\varrho(x_1, x_2, x_3) = C \frac{1}{\sqrt{x_1}} \frac{1}{\sqrt{x_2}} \frac{1}{\sqrt{x_3}} \delta(1-x_1-x_2-x_3)$$

where the constant  $C$  is determined from the normalization to unity of the probability function  $\varrho$ .

Calculations of the rapidity distribution were performed by Sukhatme [20]. Tran and I have computed recently the multiplicity distributions. Although the applicability



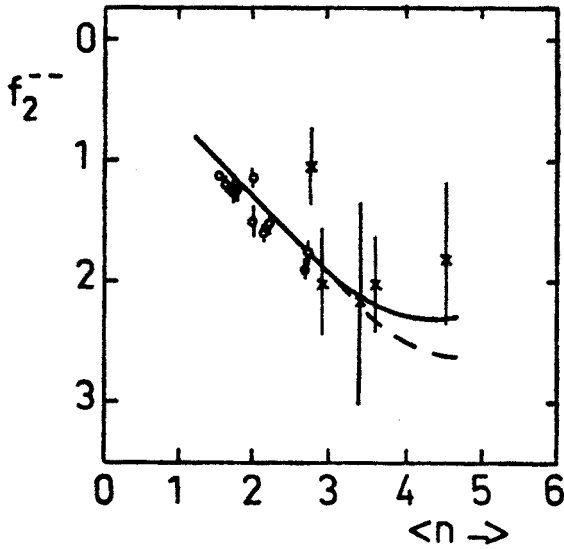


Fig. 8. The correlation factor  $f_2^{--}$  vs  $\langle n \rangle$  in the dual parton model, compared with experimental data. The dashed line is the result obtained with the three-chain diagram. The full line is obtained when multi-chain diagrams are included

of the model at low energies may be dubious, it is interesting that one obtains for the correlation factor  $f_2^{--}$  the result shown in Fig. 8. This is the only model I know in which one obtains the characteristic turn over of  $f_2^{--}$  as a function of  $\langle n \rangle$ .

### 5. Soft hadron-nucleus and nucleus-nucleus

The dual parton model can be generalized in a rather straightforward way to study multi-hadron production in hadron-nucleus and nucleus-nucleus collisions [8c, 21]. The leading and next-to-leading diagrams for proton-nucleus interactions are shown in Figs 9. Fig. 9a corresponds to a single inelastic collision of the proton with one nucleon in the target (the  $A-1$  remaining nucleons being spectators). As the corresponding diagrams for a  $p-p$  interaction, it contains two ( $q-q\bar{q}$ ) chains of produced hadrons. Fig. 9b

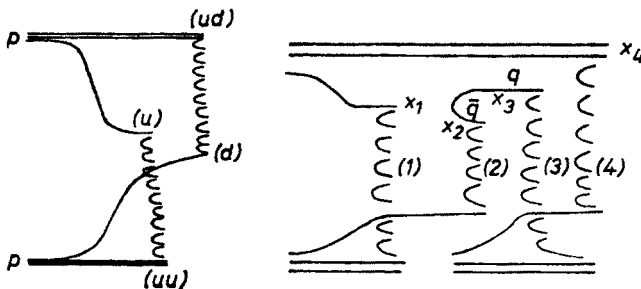


Fig. 9. Single and double inelastic collision diagrams in proton-nucleus interactions

corresponds to two inelastic collisions with two different nucleons from the target,  $A - 2$  nucleons being spectators. In this case there are four chains of produced hadrons. In general a diagram corresponding to  $\mu$  inelastic collisions will contain  $2\mu$  chains. Since both momentum distribution and fragmentation functions are the same as in the case of a hadron-hadron collision, the properties of the hadronic system can be computed with no freely adjustable parameter. The generalization to nucleus-nucleus collisions is also possible [22].

The results of the calculation of the rapidity distributions in  $p-Xe$ ,  $p-Ar$  [8c] and  $\alpha-\alpha$  [22] interactions are shown in Figs. 10 and 11 together with experimental data.

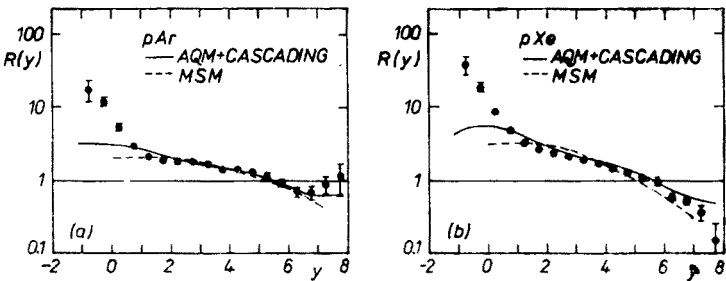


Fig. 10. Charged particle rapidity distributions for  $p-Ar$  and  $p-Xe$  at 200 GeV/c [35]. The line is the theoretical prediction

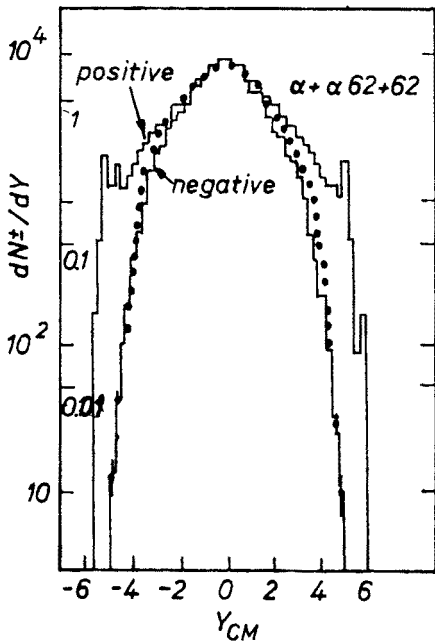


Fig. 11. Rapidity distributions of positive and negative particles in  $\alpha-\alpha$  collisions at  $\sqrt{s_{NN}} = 31$  GeV [36]. The dotted line is the calculation for negative particles

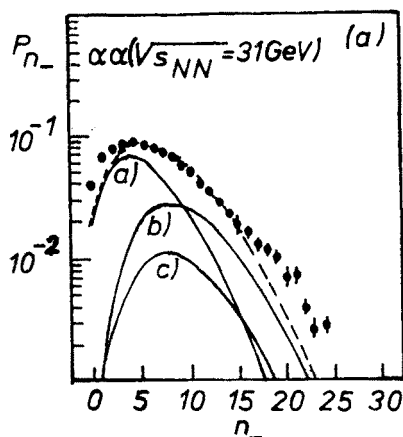


Fig. 12. The topological cross-sections for negative particles vs  $\langle n^- \rangle$ . The curve is the theoretical calculation [25]. The experimental points are preliminary data. In fact, the new data are in very good agreement with the theoretical curve [37]

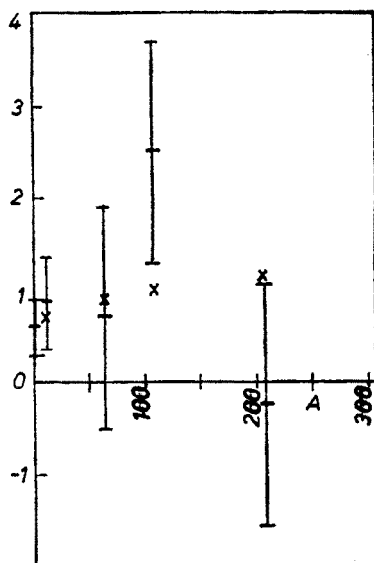


Fig. 13. Experimental data for the difference of average charged multiplicities in  $\bar{p}$ -nucleus and  $p$ -nucleus collisions, compared with the results of a theoretical model [26]

The multiplicity distributions for  $p$ -Xe and  $p$ -Ar [23] and for  $\alpha$ - $\alpha$  [24, 25] have also been computed. They are substantially broader than in the case of a proton-proton collision, in agreement with experiment (see Fig. 12).

Pajares and Ramallo [26] have generalized the model to annihilation processes on nuclei. Their main result is shown in Fig. 13.

### 6. Cross-sections

So far we have considered physical quantities such as  $dn/dy = (1/\sigma_{in})d\sigma/dy$  which are normalized to  $\sigma_{Tot}$  (or  $\sigma_{in}$ ). How to compute  $\sigma_{Tot}$ ,  $d\sigma/dt$  etc.? As mentioned above there is a one-to-one correspondence between the various terms in the  $1/N$  expansion and the diagrams of Reggeon field theory. The latter has been used both in its perturbative and non-perturbative forms to compute total, elastic and diffractive cross-sections. However, in contrast with the quantities considered in the previous sections, here there are a few freely adjustable parameters. For instance, the absolute value of  $\sigma_{Tot}$  cannot be computed.

A comprehensive analysis in the perturbative approach, which leads to a good description of the data up to ISR energies, can be found in Refs [27] and [28]. Can these calculations be extended to  $\sqrt{s} = 540$  GeV and more generally is the perturbative reggeon calculus valid at such energies? Pajares et al. [29] have used the parameters obtained in Ref. [27] to compute the values of the cross-sections at  $\sqrt{s} = 540$  GeV. They find  $\sigma_{Tot}^{pp} \sim 66$  mb. They also find that the diagrams which had been neglected at ISR energies are still very small at SPS energies. However, when computing  $\sigma_D$  one has problems of convergence of the perturbative series. More work is needed to determine whether it is possible to find

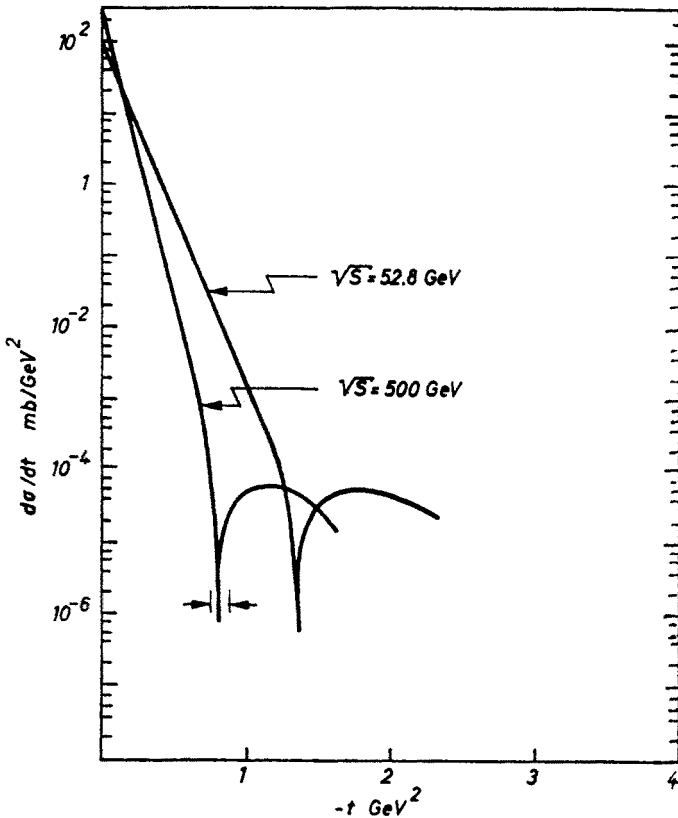


Fig. 14. Critical Pomeron prediction [31] for the  $\bar{p}$ -p differential cross-section

another set of parameters which describes the experimental data up to ISR energies and for which the perturbative series for all physical quantities makes sense.

It is also possible to obtain the asymptotic behaviour of the sum of all graphs [30]. The problem is analogous to a critical phenomenon problem in Statistical Mechanics. Scaling formulae, valid at  $s \rightarrow \infty$ , are obtained using renormalization group methods. Are these formulae valid at  $\sqrt{s} = 540$  GeV?, i.e. is the leading term of the sum (at  $s \rightarrow \infty$ ) also the dominant term at  $\sqrt{s} = 540$  GeV? Phenomenological applications of the asymptotic solution have appeared recently in the literature [31]. They involve a parametrization of the non-leading terms in  $s$  (which have not been computed so far) and a determination of the parameters from a fit to the existing data. The most interesting predictions are the energy behaviour of  $\sigma_{\text{Tot}}$  and  $d\sigma/dt$  for  $p\bar{p}$ . One can see (Fig. 14) that the dip in  $d\sigma/dt$  is moving inwards when  $s$  increases. The non-leading term in  $s$ , as parametrized in Ref. [31], turns out to be negligibly small at  $\sqrt{s} = 540$  GeV. The measurement of  $d\sigma/dt$  at the SPS will thus provide a rather clean test of the theory<sup>3</sup>.

Let me also mention that it is very interesting to compare the so-called rigorous results (based essentially on unitarity, analyticity and crossing) with the  $p\bar{p}$  collider data. A comprehensive review was presented by A. Martin at the Paris meeting.

## 7. Hadron masses

A DTU approach to the calculation of both meson [32] and baryon masses [33] exists. One can compute all the masses of all pseudo-scalar and vector  $q\bar{q}$  states (with  $q = u, d, s, c$  and  $b$ ). Four masses are used as input ( $m_q, m_\phi$  (or  $m_{K^*}$ ),  $m_\psi$  and  $m_T$ ). One can also compute the masses of all the lowest  $qqq$  states with  $q = u, d$  using as sole input the  $q$  mass. The effect of sea quark loops is included from the very beginning. In contrast to other approaches a small  $m_\pi^2/m_q^2$  ratio arises quite naturally.

## 8. Summary

Presently we do not know anything about hadronization from QCD. All models for hadronization are classical ones. Hadronization plays a crucial role even in hard processes at present values of  $Q^2$ . For low  $p_T$  physics, not even the basic mechanism at the origin of multi-hadron production is known from QCD.

The dual parton model proposes a mechanism based upon very general topological arguments. This model has all the nice properties of an  $S$ -matrix theory and provides a unified and comprehensive description of low  $p_T$  hadron-hadron, hadron-nucleus and nucleus-nucleus multi-hadron production, both in the central and fragmentation regions. The complicated mechanism of multi-particle production in these processes is reduced to "elementary"  $q\bar{q}$ ,  $qq\bar{q}$  and  $qq\bar{q}\bar{q}$  color separation mechanisms.

---

<sup>3</sup> Note, however, that the leading term itself is calculated using some perturbative treatment (the so-called  $\epsilon$ -expansion). So far, only the first term in this expansion has been calculated. A complete calculation of the second term is in progress [32]. It will be interesting to see how big is the effect of this second term in  $d\sigma/dt$ .

However, other models propose very different mechanisms. These models are also successful in describing the production processes, at least in the fragmentation regions. Accurate comparisons of the predictions of the various models in the central region are still lacking. Hopefully these comparisons will be very important in distinguishing among the various models.

## REFERENCES

- [1] K. Konishi, A. Ukawa, G. Veneziano, *Phys. Lett.* **78B**, 243 (1978); *Nucl. Phys.* **B157**, 45 (1979).
- [2] For recent reviews see U. Sukhatme, in *Partons in Soft Hadronic Physics*, Proc. Europhysics Study Conf., Erice Italy (1981), ed. R. Van de Walle and review article in Proc. XIII International Symposium on Multiparticle Dynamics, Volendam, The Netherlands (1982), where references to the original publications can be found.
- [3] See D. Amati, A. Bassetto, M. Ciafaloni, G. Marchesini, G. Veneziano, *Nucl. Phys.* **B173**, 429 (1980) and references therein.
- [4] (a) For recent reviews see A. Dar, in *Partons in Soft Hadronic Physics* [2] and A. Bialas, in Proc. Volendam Symposium [2]; b) R. Hwa, contributions to the Proc. of Erice and Volendam [2].
- [5] F. Low, *Phys. Rev.* **D12**, 163 (1975); S. Nussinov, *Phys. Rev. Lett.* **34**, 1286 (1975).
- [6] J. F. Gunion, in *Partons in Soft Hadronic Processes* [2]; J. F. Gunion, G. Bertsch, *Phys. Rev.* **D25**, 746 (1982).
- [7] B. Andersson, G. Gustafson, I. Holgerdsson, O. Mansson, *Nucl. Phys.* **B178**, 242 (1982). See also De Wolf in Proc. Volendam [2].
- [8] (a) A. Capella, U. Sukhatme, C. I. Tan, J. Tran Thanh Van, *Phys. Lett.* **81B**, 68 (1979); (b) A. Capella, U. Sukhatme, J. Tran Thanh Van, *Part. and Fields* **3**, 329 (1980); (c) A. Capella, J. Tran Thanh Van, *Part. and Fields* **10**, 249 (1981); *Phys. Lett.* **93B**, 946 (1980); (d) A. Capella, J. Tran Thanh Van, *Phys. Lett.* **114B**, 450 (1982); (e) G. Cohen-Tannoudji, A. El Hassouni, J. Kalinowski, O. Napoly, R. Peschanski, *Phys. Rev.* **D21**, 2689 (1980); (f) H. Minakata, *Phys. Rev.* **D20**, 1656 (1979).
- [9] G. Veneziano, *Nucl. Phys.* **B74**, 365 (1974); **B117**, 519 (1976); Chan Hong Mo et al., *Nucl. Phys.* **B86**, 470 (1975); **B92**, 13 (1975); G. Chew, C. Rosenzweig, *Nucl. Phys.* **B104**, 290 (1976); *Phys. Rep.* **41C**, 263 (1978).
- [10] G. Preparata et al., preprints BARI-GT/80-09 and 81-05.
- [11] See G. Veneziano, in Proc. XII Rencontre de Moriond 1976, ed. J. Tran Thanh Van and GIF lectures 1977; Girardi GIF lectures, 1976; G. 't'Hooft, *Nucl. Phys.* **B72**, 461 (1974).
- [12] P. Aurenche, F. Bopp, *Phys. Lett.* **114B**, 363 (1982).
- [13] (a) A. B. Kaidolov, preprint ITEP-50 (1982); (b) A. B. Kaidalov, K. A. Ter-Martirosyan, preprint ITEP-51 (1982).
- [14] A. Pagnamenta, U. Sukhatme, *Part. and Fields* **14**, 79 (1982).
- [15] (a) K. Fialkowski, A. Kotanski, *Phys. Lett.* **107B**, 132 (1981); (b) *Phys. Lett.* **115B**, 425 (1982).
- [16] UAI Collab. results, in Proc. of VIth European Symposium on  $N-\bar{N}$  and  $q-\bar{q}$  interactions, Santiago de Compostela, Spain (1982).
- [17] A. Capella, A. Krzywicki, *Phys. Rev.* **D18**, 3357 (1978); *Phys. Lett.* **B67**, 84 (1977).
- [18] A. Capella, J. Tran Thanh Van, in preparation.
- [19] UA5 Collab. results, in Proc. of VIth European Symposium on  $N-\bar{N}$  and  $q-\bar{q}$  interactions, Santiago de Compostela, Spain (1982).
- [20] U. Sukhatme, *Phys. Rev. Lett.* **45**, 5 (1980); D. R. Ward, in Proc. of Vth European Symposium on  $N-\bar{N}$  interactions, Bressanone, Italy (1980), ed. I.N.F.N., Padova.
- [21] W. W. Chao, C. Chiu, Z. He, D. M. Tow, *Phys. Rev. Lett.* **44**, 518 (1980).
- [22] A. Capella, J. Kwiecinski, J. Tran Thanh Van, *Phys. Lett.* **108B**, 347 (1982).
- [23] A. Capella, J. Tran Thanh Van, in Proc. of the XVI Rencontre de Moriond (1981), ed. J. Tran Thanh Van.

- [24] A. Capella, C. Pajares, A. Ramallo, J. Tran Thanh Van, in preparation.
- [25] W. Q. Chao, H. J. Pirner, *Part. and Fields* **14**, 165 (1982).
- [26] C. Pajares, A. Ramallo, *Phys. Lett.* **107B**, 373 (1981).
- [27] A. Capella, J. Kaplan, J. Tran Thanh Van, *Nucl. Phys.* **B97**, 493 (1975).
- [28] M. S. Dubovikov et al., *Nucl. Phys.* **B123**, 147 (1977).
- [29] C. Pajares, private communication.
- [30] For a review see H. D. I. Abarbanel, J. B. Bronzan, R. L. Sugar, A. R. White, *Phys. Rep.* **LIC**, 119 (1975).
- [31] J. Baussel, M. Feingold, M. Moshe, *Nucl. Phys.* **B198**, 13 (1982).
- [32] Private communication from Bartels and Dash.
- [33] L. A. Balazs, Purdue Univ. Preprint (1982); *Phys. Rev.* **D20**, 2331 (1979); A. Kaidalov, preprint ITEP-78 (1980).
- [34] L. A. Balazs, B. Nicolescu, *Part. and Fields* **6**, 269 (1980); Purdue Univ. preprint (1982).
- [35] See I. Derado, Proc. 17th Rencontre de Moriond (1982), ed. Tran Thanh Van.
- [36] See M. Faessler, Proc. Moriond [35].
- [37] See M. Faessler, Proc. Volendam [2].